



## Biomechanics of an interlinked suture anchor rotator cuff repair in a human cadaveric model



Klevis Aliaj, BS <sup>a,b</sup>, Heath B. Henninger, PhD <sup>a,b</sup>, Jean-Olivier E. Tétreault-Paquin, MD <sup>c</sup>, Mark H. Getelman, MD <sup>d</sup>, Joseph P. Donahue, MD <sup>c,\*</sup>

<sup>a</sup> Harold K. Dunn Orthopaedic Research Laboratory, Department of Orthopaedics, University of Utah, Salt Lake City, UT, USA

<sup>b</sup> Department of Bioengineering, University of Utah, Salt Lake City, UT, USA

<sup>c</sup> SOAR (Sports, Orthopedic, and Rehabilitation), Redwood City, CA, USA

<sup>d</sup> Southern California Orthopaedics Institute, Van Nuys, CA, USA

### ARTICLE INFO

#### Keywords:

Shoulder  
rotator cuff repair  
interlinked  
suture anchor  
cyclic testing  
gapping  
failure testing

*Level of evidence:* Basic Science Study,  
Biomechanics

**Background:** The purpose of this study was to evaluate the initial fixation of a transosseous-equivalent rotator cuff repair and an interlinked medial repair, quantifying the cyclic and failure loading properties of each construct.

**Methods:** Twenty-four human cadaveric shoulders from 12 matched pairs were dissected, and full-thickness supraspinatus tears were created. In each pair, 1 side was repaired with a transosseous-equivalent repair (control) and the other, with an interlinked repair. All specimens were cycled to 1 MPa of effective stress at 1 Hz for 500 cycles, and gap formation was recorded with a digital video system. All samples were then loaded to failure, and the ultimate load and displacement and modes of failure were recorded.

**Results:** The interlinked repair showed a decrease in the amount of construct gapping after cycle 50 and in peak construct gapping compared with the control group (control,  $3.4 \pm 0.9$  mm; interlinked,  $2.5 \pm 0.8$  mm;  $P = .048$ ). The interlinked repair also showed a higher ultimate load to failure (control,  $318.7 \pm 77.9$  N; interlinked,  $420.6 \pm 93.7$  N;  $P = .007$ ). No other significant differences were detected between constructs for preparation or testing metrics.

**Conclusions:** The interlinked repair, in which 1 continuous suture linked the medial anchors, showed decreased construct gapping and increased ultimate load to failure compared with the control construct. This study establishes the biomechanical validity of the new interlinked repair construct compared with a previously validated construct.

© 2019 The Author(s). Published by Elsevier Inc. on behalf of American Shoulder and Elbow Surgeons. This is an open access article under the CC BY-NC-ND license (<http://creativecommons.org/licenses/by-nc-nd/4.0/>).

Rotator cuff tears remain a therapeutic challenge for orthopedic surgeons despite continual improvement in surgical techniques and instruments. In particular, large and massive tears show significant failure rates after surgical repair.<sup>7,12</sup> Tendon tearing through sutures is the predominant mode of failure for rotator cuff repairs, with most failures occurring during the first 6 months after surgery.<sup>9,17,20,28</sup>

The repair should restore the humeral rotator cuff footprint area, provide tendon-to-bone compressive forces, and achieve overall mechanical stability to encourage healing.<sup>23</sup> A variety of surgical techniques attempt to optimize the aforementioned repair criteria,

and the relative merits of different design considerations have been quantified. It has been shown that maximizing the number of sutures crossing the tendon leads to decreased gap formation and increased ultimate strength of the repair.<sup>3,19</sup> Increasing the number of anchors offers no biomechanical advantage when the number of sutures is kept constant.<sup>19</sup> Smaller horizontal mattress stitches have the advantage of fixing the tendon more tightly at the cost of decreased ultimate strength, whereas larger horizontal stitches have greater ultimate strength but increased gap formation and strain.<sup>32</sup>

Medial anchor linkage has been shown to improve the medial load-sharing capacity and increase repair strength and contact pressure with varying techniques including the diamondback repair, double-pulley technique, Roman bridge technique, tendon trap technique, and medial inter-implant mattress technique.<sup>1,5,8,11,21,30</sup> All of these surgical procedures use varying methods to link the medial row of anchors; however, they introduce static fixation points between the 2 medial anchors. The static

Use of human cadaveric tissues for biomechanical testing is exempt per Institutional Review Board No. 11755 of the University of Utah ("Biomechanical Testing of Orthopaedic Devices Using Descendent Tissue Models").

\* Corresponding author: Joseph P. Donahue, MD, SOAR (Sports, Orthopedic, and Rehabilitation), 500 Arguello St, Ste 100 Redwood City, CA 94063, USA.

E-mail address: [donahue@stanfordalumni.org](mailto:donahue@stanfordalumni.org) (J.P. Donahue).

<https://doi.org/10.1016/j.jses.2019.02.002>

2468-6026/© 2019 The Author(s). Published by Elsevier Inc. on behalf of American Shoulder and Elbow Surgeons. This is an open access article under the CC BY-NC-ND license (<http://creativecommons.org/licenses/by-nc-nd/4.0/>).

fixation points could prevent the linked suture from sliding freely, thus inhibiting load sharing and even tensioning between the 2 anchors of the medial row. Furthermore, unless additional fixation points (ie, knots) are introduced, additional anchors cannot be linked together.

An interlinked rotator cuff repair system provides a method for anchors to share tension evenly. This is accomplished by using an anchor and suture technique that allows the same running suture to connect 2 or more anchors without the necessity of tying sutures together between adjacent anchors. Qualitative observation has shown that the suture is free to slide within the eyelet of each anchor, and each anchor can act as a load-sharing pulley. Multiple anchors (up to 4 in our experience) can be linked with the same suture, allowing for a variety of repair techniques to be performed.

Although linked rotator cuff repairs have been investigated before, no data characterizing the biomechanics of a repair interlinked with a continuous length of suture currently exist. As such, we investigated the biomechanical properties of the interlinked repair by comparing it with a popular transosseous-equivalent repair frequently used in rotator cuff repair surgery. We hypothesized that the interlinked repair would have comparable gap formation, failure loads, and failure displacement to the transosseous-equivalent repair during cyclic and failure loading.

## Methods

### Specimen preparation

Twelve pairs of fresh-frozen human male cadaveric shoulders (aged  $71 \pm 6$  years) with no history of shoulder pathology, injury, or surgery as determined from tissue donor summaries (United Tissue Network, Norman, OK, USA, and ScienceCare, Phoenix, AZ, USA) were selected for the study. Prior to preparation, the specimens were thawed at room temperature for 24 hours. Normal saline solution was used to continually hydrate the tissue during the dissection and the experiment.

All soft tissues, with the exception of the rotator cuff and glenohumeral capsule, were removed from the humerus and scapula. Subsequently, the humeri were disarticulated from the scapulae by carefully dissecting around the rotator cuff muscle bellies and capsules. The remaining subscapularis, supraspinatus, infraspinatus, and teres minor tendons and their muscle bellies were preserved on the humeral head.

Next, the anterior and posterior margins of the supraspinatus tendon were identified, and the remaining cuff tendons were dissected from their humeral insertions. This dissection technique may have captured some fibers of the infraspinatus tendon at its shared insertion with the supraspinatus, but the architecture of the tendon was variable between specimens. The only reliable landmark to guide resection was the posterior edge of the supraspinatus as it proceeded laterally to the insertion. On the distal surface of the supraspinatus, any remaining adherent capsular tissue was finely dissected away from the tendon. The supraspinatus was then bluntly dissected at its insertion. The cross-sectional area of the supraspinatus tendon was computed by multiplying the average width by the average thickness of the tendon. The width and thickness of the tendon at the planned level of the repair were recorded 3 times with digital calipers (150 mm Mitutoyo 500; Mitutoyo, Aurora, IL, USA) and averaged.

### Rotator cuff repair constructs

A coin flip was used to determine which specimen within a pair received the control or interlinked rotator cuff repair. The control

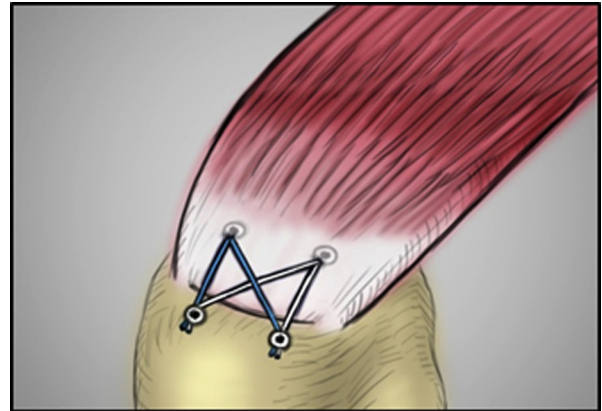


**Figure 1** Schema of control double-row transosseous-equivalent rotator cuff repair.

construct consisted of a transosseous-equivalent, 4-anchor, double-row rotator cuff repair (SpeedBridge; Arthrex, Naples, FL, USA) (Fig. 1). The medial row was placed with two 4.75-mm SwiveLock C medial-row anchors (Arthrex) loaded with FiberTape (Arthrex). Both tails of the tape were passed simultaneously through the tissue. The free tails were then fixed laterally using 2 more 4.75-mm SwiveLock anchors.

The contralateral shoulder received a transosseous-equivalent, 3-anchor repair using an interlinked anchor technique (Fig. 2). The medial row consisted of 2 double-loaded 5.5-mm anchors (Stabilynx, Menlo Park, CA, USA). The limbs of 1 suture from each anchor were passed in a horizontal mattress fashion. Each suture had a built-in loop near the end, which was used to shuttle the end of 1 suture from 1 anchor through the other anchor, creating a free-sliding running suture through both anchors. The other suture limbs were passed in a horizontal mattress fashion medial to the bridge, allowing the bridge to also act as a rip stop for these mattress sutures. All of the sutures were tied, and the tails were fixed laterally with 1 knotless anchor (4.75-mm SwiveLock anchor).

In both repair groups, the first medial-row anchor was placed 5 mm posterior to the bicipital groove just lateral to the articular margin, and the second anchor was placed 15 mm posterior to the first anchor. Anchors were inserted at  $45^\circ$  to the bone surface. Placing the anchors immediately adjacent to the articular cartilage provided a uniform landmark, which was consistent with the site of greatest bone strength.<sup>33,34</sup> This layout standardized each repair and anchor location.<sup>26</sup>

### Mechanical testing

Each humerus was transected at the midshaft and clamped to the base on an Instron system (1331 Load Frame with model 8800 controller; Instron, Norwood, MA, USA) as described previously.<sup>26,29</sup> The supraspinatus muscle belly was secured to the Instron actuator via a custom cryoclamp. The fixation apparatus was aligned so that the angle between the supraspinatus muscle belly and the humeral shaft was  $135^\circ$ .<sup>2</sup>

A material testing system was used to apply cyclic and failure loads to the repair constructs while a 1-kilonewton load cell (Dynacell, model 2527-130; Instron) monitored the applied force. A preload force targeted to generate 0.1 MPa of equivalent stress was applied to each construct in preparation for cyclic loading. Within a pair of humeri, the cross-sectional area of the tendon was averaged and multiplied by 0.1 MPa of stress to obtain the preload force. This strategy was used to normalize loads between tendons of varying size (cross-sectional area) between donor specimens. The construct was allowed to undergo stress and relaxation at the displacement

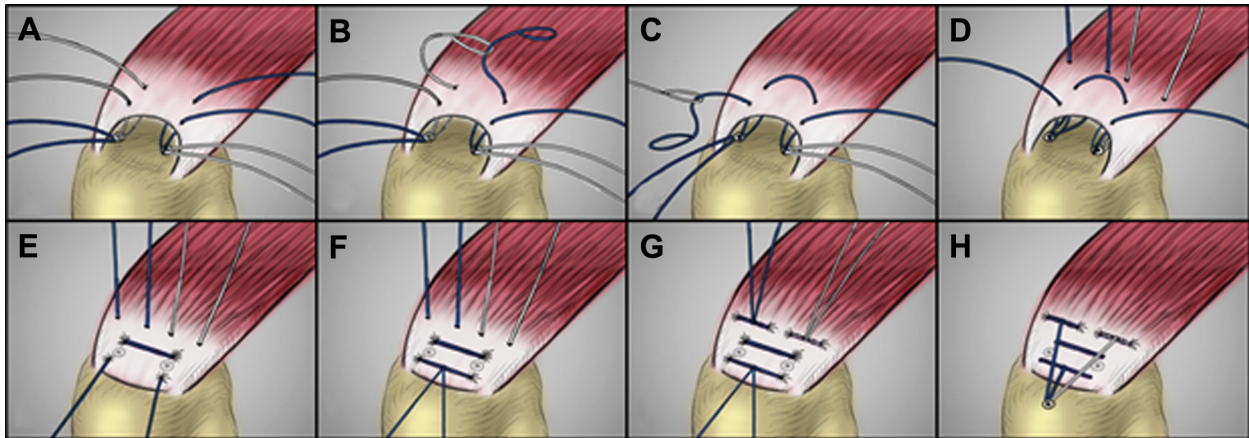


**Figure 2** Schema of interlinked medial-row rotator cuff repair. (A) Both legs of 1 suture from each medial-row anchor were passed through the tendon. (B) One free end of the anterior suture (blue) was looped through 1 leg of the posterior suture (white). (C) The free end of the anterior suture (blue) was shuttled through the tendon and posterior anchor by the posterior suture (white). (D) Both legs of the remaining suture from each anchor were passed through the tendon in preparation for a horizontal mattress stitch medial to the interlinked bridge. (E) The interlinked suture (blue) was tensioned to lay down the medial-row bridge, evenly distributing pressure on the tendon between both medial-row anchors. (F) The interlinked suture (blue) was tied to complete the lateral bridge, with a single suture distributing pressure on both rows between the 2 anchors. (G) The horizontal mattress stitches were tied medial to the medial bridge to act as a rip stop. (H) All free ends were laid down and secured to the lateral anchor.

required to reach the preload force for 120 seconds, and then the cyclic loading test was started. The cyclic loading consisted of five hundred 1-Hz cycles of a triangular displacement waveform that varied the applied stress between 0.1 and 1 MPa, again calculated from the cross-sectional area of the respective pair of shoulders. After cyclic loading and a 1-second pause, the 0.1-MPa preload stress was reapplied to ensure all constructs began failure loading from the same initial conditions. Thereafter, the constructs were pulled to failure at a rate of 1.0 mm/s. The mechanical testing protocol was adapted from previous studies of rotator cuff repairs.<sup>4,26,29</sup>

#### Tissue and construct displacement tracking

Tissue and construct displacement was tracked using DMAS (Digital Motion Analysis System, version 6.5; Spicetek, Maui, HI, USA). Three rows of 2-mm black beads were adhered onto the bone (immediately inferior to the lateral anchors on the greater tuberosity), tendon (just medial to the medial row of anchors and suture), and muscle belly (approximately halfway between the medial anchors and the bottom of the cryoclamp) using cyanoacrylate. Hereafter, we refer to the beads on the bone as the “bone markers” and the beads closest to the medial anchors as the “construct markers.” By use of a digital camera with a resolution of  $1360 \times 1024$  pixels (Prosilica GC1350 Gigabit Ethernet; Allied Vision Technologies, Exton, PA, USA), these markers allowed tracking of displacement between bone and construct, as well as between construct and muscle. After calibration using DMAS, a 0.1% field-of-view accuracy—corresponding to less than 0.05 mm—was achieved.

The marker position was recorded for 3 consecutive cycles at cycles 1, 10, 50, 100, 200, 300, 400, and 500. Construct gapping was defined as the relative difference between the maximum and minimum displacement of the construct markers and bone markers, averaged among the 3 markers within each row. Tissue deformation was similarly defined as the displacement between the tissue and construct markers. Specimens that experienced more than 5 mm of construct gapping were considered to have failed during cyclic testing.<sup>4,6</sup>

Marker displacement was recorded continuously throughout failure testing, and 3 measurements were computed. Maximum failure load was defined as the peak load after which the tissue first

experienced a sharp drop in the amount of load that it supported. The captured videos were used to correlate the maximum failure load to the failure mode. For example, we assessed whether the failure load occurred at the same time as the tissue began to fail or whether an anchor started to dislodge from the bone. Maximum failure stiffness was defined as the point with the greatest increase in force per unit displacement prior to the failure load being reached. Maximum stiffness was computed by fitting a linear regression model of 40 data points centered on the point that had the greatest derivative of force with respect to displacement. Failure displacement was then defined as the construct gap at the failure load.

#### Statistical analysis

To determine an appropriate sample size, an a priori power analysis was conducted based on the work of Kullar et al.<sup>22</sup> and Montanez et al.<sup>29</sup> A matched-pair, 2-tailed power analysis (calculated in G\*Power, version 3.1<sup>10</sup>) showed that to distinguish between cyclic gapping and failure load differences measured by Kullar et al with a significance of  $P \leq .05$  and power of 0.8, a sample size of 8 matched pairs of humeri was needed. The same analysis was conducted for data from Montanez et al, which showed that a sample size of 12 was needed to distinguish the measured differences in maximum failure loads. A power analysis was not conducted on the cyclic gapping data measured by Montanez et al because no significant differences were measured between the 2 populations. On the basis of the power analysis, a conservative sample size of 12 pairs of humeri was selected to account for tissue rejection during dissection and ensure at least 8 pairs were tested.

Comparisons between constructs, as well as between construct gapping and tissue deformation within a construct, were carried out using paired *t* tests in which  $\alpha = .05$ . All data are presented as mean  $\pm$  standard deviation unless otherwise noted.

#### Results

We tested 10 of 12 pairs of specimens procured for the study because irreparable rotator cuff tears were discovered in at least 1 shoulder of 2 pairs during preparation. No partial tears or other signs of degeneration were detected in any of the other cadaveric specimens during dissection and preparation. Both the control and interlinked repairs were placed in 5 left and 5 right humeri. No

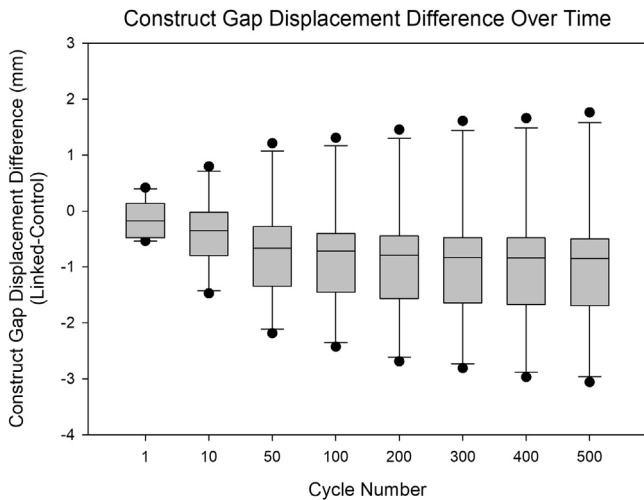


**Figure 3** Difference in construct gapping between control and interlinked repairs during cycling testing (Construct gapping difference = Interlinked – Control). The shaded boxes encompass the 25th to 75th percentiles, the solid lines within the boxes indicate the median values, and the whiskers indicate the 10th to 90th percentiles. Outliers are indicated (●). Over the course of cyclic testing, the interlinked repair group displayed less construct gapping than the control group. By the 50th cycle, the difference in construct gapping became significant.

significant differences in specimen width, thickness, and cross-sectional area were found between the control and interlinked repair groups ( $P = .055$ ,  $P = .103$ , and  $P = .066$ , respectively).

None of the specimens in our study reached the cyclic construct gapping failure point of 5 mm. After cycle 50, a significant difference in the amount of construct gapping was noted between the control and interlinked repair groups (Fig. 3). Peak construct gapping was significant between constructs, but tissue deformation did not differ by group (Table I). Construct gapping was consistently greater than tissue deformation ( $P \leq .001$ ). This finding showed that, during cyclic testing, the majority of the deformation was encompassed within construct gapping and that we indeed tested the properties of each repair vs. the properties of the muscle tissue.

When undergoing testing to failure, 2 specimens experienced muscle belly failures that did not adequately load the constructs to failure. These 2 pairs were excluded from further analysis because they would not allow for proper comparison of maximum load and stiffness values between the 2 constructs. The width, thickness, and area of each of the remaining 8 pairs, excluding muscle belly failures, did not differ between constructs (Table II).

The control repair group failed via either the lateral anchor pulling out of the bone or the tissue tearing at the medial anchor suture line (Table III). The interlinked repair group failed primarily through pullout of the medial anchors from bone.

We found a significant difference in the maximum failure load supported by the interlinked repair vs. the control repair (Table IV). However, no significant difference in maximum stiffness and construct gapping at maximum load was noted between the interlinked and control groups.

**Discussion**

In this study, we compared a traditional transosseous-equivalent repair and a medially interlinked repair to determine differences in initial fixation strength between the 2 constructs. Our hypothesis that no differences would exist between constructs was rejected, because the interlinked repair had decreased construct gapping and increased ultimate load to failure compared with the control construct.

**Table I**  
Peak construct gapping and tissue deformation at cycle 500

Construct	Construct gap, mm	Tissue deformation, mm
Control	3.4 ± 0.9	0.6 ± 0.3
Interlinked	2.5 ± 0.8	0.6 ± 0.3
P value	.048	.696

Initial fixation strength of rotator cuff repairs, especially as it relates to cyclic loading, is a primary consideration when evaluating a rotator cuff repair.<sup>6,17,28</sup> Although no specimens reached the 5-mm threshold for failure during cycling, the interlinked rotator cuff repair construct showed a significantly lower amount of construct gapping after cycle 50 and showed less peak construct gapping after 500 cycles compared with the control group. This finding demonstrates that the interlinked repair system improved fixation of the tendon onto the bone compared with the control construct. This is advantageous not only because it provides greater initial fixation strength but also because it more consistently maintains the original footprint of the tendon over the bone as established during surgery.

Load-to-failure testing showed failure modes either at the tendon-suture interface or at the anchor site. Although the load at each anchor was not measured directly, it can be inferred from the failure modes: Many specimens in the control group failed by lateral anchor pullout (ie, higher loads transferred laterally); in contrast, among interlinked specimens, the medial anchors failed most of the time (ie, medial anchors bore the higher loads). This finding suggests that the force transmitted in the interlinked repair is weighted toward the medial anchors where soft-tissue fixation occurs, as opposed to anchors inserted lateral to the tendon. Given that interlinked constructs had only a single lateral anchor, it would be assumed that the lone anchor would pull out more reliably than in controls if the same loads were transferred laterally. Bone density and load to failure decline as the anchor insertion site moves laterally and distally in the humeral head,<sup>33,34</sup> making lateral anchor insertion sites weaker and more prone to tendon-bone gap formation.

Regardless, the loads in both groups were likely supra-physiological. The supraspinatus failed above 800 N when intact tendons were tested to failure.<sup>18,25</sup> Simulations use forces between 40 and 200 N to actuate the supraspinatus during arm elevation.<sup>14–16,27</sup> Failure forces in our study ranged from 191 to 534 N, illustrating that both constructs performed predominantly beyond their expected clinical demands. No data for the material properties of an acutely or chronically torn supraspinatus are available, but they would be expected to be considerably lower than intact healthy tendon properties and to be a source of failure before the construct.

Stiffness, however, is not significantly different between the medial and lateral regions of the humeral head.<sup>33,34</sup> Our results show that maximum construct stiffness is not significantly different between the interlinked and control repairs. Thus, the increased maximum load-to-failure values but similar stiffness

**Table II**  
Comparison of supraspinatus tendon sizes between repair groups (8 pairs), excluding muscle belly failures

Construct	Tendon width, mm	Tendon thickness, mm	Cross-sectional area, mm <sup>2</sup>
Control	25.7 ± 2.5	4.7 ± 0.7	122.2 ± 23.5
Interlinked	25.1 ± 2.5	4.4 ± 0.5	111.4 ± 19.5
P value	.134	.214	.158

**Table III**  
Failure mode summary for control and interlinked repair groups

Pair No.	Control	Interlinked
1	Dual lateral anchor pullout	Dual medial anchor pullout
2	Anterior lateral anchor pullout	Dual medial anchor pullout
3	Tissue tearing at suture line	Dual medial anchor pullout
4	Dual lateral anchor pullout	Dual medial anchor pullout
5	Tissue tearing at suture line	Tissue tearing at suture line, posterior medial anchor pullout
6	Dual medial anchor pullout	Dual medial anchor pullout
7	Tissue tearing at suture line, posterior lateral anchor pullout after preload	Tissue tearing at suture line, propagated to MTJ
8	Tissue tearing at suture line	Tissue tearing at suture line, propagated to MTJ

MTJ, musculotendinous junction.

values again signal that force bearing is medialized in the interlinked repair. Because cycling tensioning leads to stiffening of the construct under testing through cinching of the suture, knots, and tendon, the maximum stiffness recorded was correlated to the point at which maximum force was applied during cyclic testing ( $R^2 = 0.944$ , data not shown). A comparison of average stiffness and stiffness at 175 N (greater than any applied cyclic loading force) was further analyzed, showing no significant difference between the 2 repairs, with  $P = .337$  and  $P = .659$ , respectively.

As expected, construct gapping at failure was also not significantly different between the 2 repairs. Assuming that the 2 constructs have similar structural properties (and do not fail during cyclic testing), construct gapping at failure is a measure of the composite properties of the underlying bone, soft tissue, and muscle. Because a matched-pair experimental design was used, construct gapping at failure was expected to not be significantly different between the 2 repairs because comparable cadaveric specimens were consistent between groups.

The tendon width, thickness, and cross-sectional area of the samples used in this study were comparable to those in other studies with similar experimental protocols.<sup>22,26,29</sup> Likewise, peak cyclic construct gapping was comparable to that in previous studies. The ultimate failure load for both constructs was lower in our study but still suprphysiological. Previous studies have reported ultimate failure loads in the range of 430 to 570 N, whereas this study found failure loads in the range of 191 to 534 N. The mean specimen age in comparable studies was 58 to 60 years, whereas the mean specimen age in this study was 71 years, which may have led to decreased failure loads in older tissues, although no clear trend arose.

Although the biomechanical integrity of a rotator cuff repair construct is important, so is its ability to encourage biological healing and blood flow. It is expected that the blood flow characteristics of the interlinked repair are comparable to those of other medial repairs. Currently, no studies exist comparing blood flow between a transosseous-equivalent, double-row rotator cuff repair

and a medially linked repair. However, it has been shown that there is no significant difference in blood flow between single- and double-row rotator cuff repairs.<sup>24</sup> A double-row rotator cuff repair provides greater compression of the tendon onto the bone laterally compared with a single-row rotator cuff repair, yet the blood flow between the 2 repairs is not statistically different. Similarly, a medially interlinked repair aims to provide more compression of the tendon onto the bone medially compared with a double-row, transosseous-equivalent repair. Future research should examine the ability of these constructs to explicitly promote blood flow in the repaired tendon footprint.

The choice of the transosseous-equivalent, double-row repair technique as a control was deliberate, given that the popular construct has a wide basis for comparison, but the constructs are inherently different. The control construct had 2 points of suture passage through the tendon whereas the interlinked construct had 8, and the increased number of suture passes through tendon, as well as medial linkage, has previously been shown to decrease gap formation and increase ultimate strength of the repair.<sup>3,19</sup> Varying the number of suture passes is not uncommon in rotator cuff repair studies evaluating new or alternative constructs.<sup>13,30,31</sup> Although increasing the number of anchors offers no biomechanical advantage when the number of sutures is kept constant,<sup>19</sup> the ability to reduce the number of anchors in the tested interlinked configuration without sacrificing construct integrity, as shown in this study, could be a cost and time savings in clinical use. There may be concern that using a single continuous strand of suture could lead to issues if the suture breaks, the knot slips, or an anchor eyelet breaks, yet these concerns are valid for any construct using suture anchors. As tested, the continuous suture was used in a load-sharing rip-stop configuration in which the medial anchors were double loaded, not unlike many other cuff repair strategies in which similar concerns of suture anchor and knot integrity are tempered by the use of additional fixation as failsafe points.

There are limitations to this study. First, it was a cadaveric study; therefore, the loading scenarios tested likely do not mimic the complex loading of the supraspinatus tendon in vivo. However, a

**Table IV**  
Comparison of maximum failure load, maximum stiffness, and construct gapping at maximum load between control and interlinked repair groups

Pair No.	Maximum failure load, N		Maximum stiffness, N/mm		Construct gapping at maximum load, mm	
	Control	Interlinked	Control	Interlinked	Control	Interlinked
1	330.5	534.3	100.1	123.5	8.3	11.9
2	268.3	360.7	100.9	110.2	5.6	5.4
3	311.3	421.3	104.3	75.2	3.7	9.0
4	191.0	258.8	76.0	98.2	4.8	2.4
5	424.5	378.2	84.4	88.8	7.4	5.4
6	422.9	517.0	103.1	111.9	5.5	7.0
7	281.9	391.3	74.2	93.9	3.3	4.6
8	319.4	503.3	88.2	102.5	6.3	6.8
Mean	318.7 ± 77.9	420.6 ± 93.7	91.4 ± 12.3	100.5 ± 15.0	5.6 ± 1.7	6.6 ± 2.9
P value		.007		.171		.344

uniform loading scenario is necessary to meaningfully compare the 2 repair constructs. Owing to the difficulty of obtaining a large number of specimens with innate rotator cuff tears, a rotator cuff defect had to be artificially created—which also may not replicate in vivo conditions given that the integrity of the tissue in most cases was good. As noted in the “Results” section, 2 pairs of specimens were excluded because their tissue quality was so degraded that meaningful comparison to the otherwise healthy tissue was not possible. Nevertheless, a comparison between the 2 repair constructs can still be drawn because similar defects were created in each specimen paired with each construct. The matched-pair experimental design also allowed us to reduce the tissue variability between the repair groups as evidenced by the fact that tendon sizes were not statistically different between the repair groups. Although there was evidence that the medial anchors in the interlinked repair supported a greater portion of the load compared with the control group, we did not have the appropriate apparatus to measure forces at each anchor. Inherent to any cadaveric study, all tests were performed at time zero of surgery, so there is no way to evaluate the biological healing of the repairs and whether that would have been influenced by the differences in the tested constructs.

## Conclusion

Cyclic and failure testing indicated that the interlinked repair, in which 1 continuous suture linked the medial anchors, had greater strength and mechanical stability than the control repair, although both were suprphysiological. This study establishes the biomechanical validity of the new interlinked repair construct.

## Disclaimer

Joseph P. Donahue is the founder of Stabilynx and has a patent issued (15/124,344), as well as patents pending (13/566,845 and 14/610,711).

Mark H. Getelman reports grants and personal fees from DePuy Mitek, Arthrex, and Smith & Nephew; research support from Rotation Medical and Histogenics; and royalties from Wolters Kluwer.

The other authors, their immediate families, and any research foundations with which they are affiliated have not received any financial payments or other benefits from any commercial entity related to the subject of this article.

## References

1. Arrigoni P, Brady PC, Burkhart SS. The double-pulley technique for double-row rotator cuff repair. *Arthroscopy* 2007;23:675.e1–4. <https://doi.org/10.1016/j.arthro.2006.08.016>.
2. Barber FA, Coons DA, Ruiz-Suarez M. Cyclic load testing of biodegradable suture anchors containing 2 high-strength sutures. *Arthroscopy* 2007;23:355–60. <https://doi.org/10.1016/j.arthro.2006.12.009>.
3. Barber FA, Herbert MA, Schroeder FA, Aziz-Jacobo J, Mays MM, Rapley JH. Biomechanical advantages of triple-loaded suture anchors compared with double-row rotator cuff repairs. *Arthroscopy* 2010;26:316–23. <https://doi.org/10.1016/j.arthro.2009.07.019>.
4. Burkhart SS, Denard PJ, Konicek J, Hanypsiak BT. Biomechanical validation of load-sharing rip-stop fixation for the repair of tissue-deficient rotator cuff tears. *Am J Sports Med* 2014;42:457–62. <https://doi.org/10.1177/0363546513516602>.
5. Burkhart SS, Denard PJ, Obopilwe E, Mazzocca AD. Optimizing pressurized contact area in rotator cuff repair: the diamondback repair. *Arthroscopy* 2012;28:188–95. <https://doi.org/10.1016/j.arthro.2011.07.021>.
6. Burkhart SS, Johnson TC, Wirth MA, Athanasiosu KA. Cyclic loading of transosseous rotator cuff repairs: tension overload as a possible cause of failure. *Arthroscopy* 1997;13:172–6.
7. Cho NS, Rhee YG. The factors affecting the clinical outcome and integrity of arthroscopically repaired rotator cuff tears of the shoulder. *Clin Orthop Surg* 2009;1:96–104. <https://doi.org/10.4055/cios.2009.1.2.96>.
8. Chung NS, Cho JH, Han KJ, Han SH, Lee DH. Tendon trap technique for rotator cuff repair. *Orthopedics* 2012;35:1035–8. <https://doi.org/10.3928/01477447-20121120-04>.
9. Cummins CA, Murrell GA. Mode of failure for rotator cuff repair with suture anchors identified at revision surgery. *J Shoulder Elbow Surg* 2003;12:128–33. <https://doi.org/10.1067/mse.2003.21>.
10. Faul F, Erdfelder E, Lang A-G, Buchner A. G\*Power 3: a flexible statistical power analysis program for the social, behavioral, and biomedical sciences. *Behav Res Methods* 2007;39:175–91. <https://doi.org/10.3758/BF03193146>.
11. Franceschi F, Longo GU, Rizzini L, Rizzello G, Maffulli N, Denaro V. The Roman bridge: a “double pulley–suture bridges” technique for rotator cuff repair. *BMC Musculoskelet Disord* 2007;8:123. <https://doi.org/10.1186/1471-2474-8-123>.
12. Galatz LM, Ball CM, Teefey SA, Middleton WD, Yamaguchi K. The outcome and repair integrity of completely arthroscopically repaired large and massive rotator cuff tears. *J Bone Joint Surg Am* 2004;86-A:219–24.
13. Garcia IA, Jain NS, McGarry MH, Tibone JE, Lee TQ. Biomechanical evaluation of augmentation of suture-bridge supraspinatus repair with additional anterior fixation. *J Shoulder Elbow Surg* 2013;22:e13–8. <https://doi.org/10.1016/j.jse.2012.10.026>.
14. Giles JW, Ferreira LM, Athwal GS, Johnson JA. Development and performance evaluation of a multi-PID muscle loading driven in vitro active-motion shoulder simulator and application to assessing reverse total shoulder arthroplasty. *J Biomech Eng* 2014;136:121007. <https://doi.org/10.1115/1.4028820>.
15. Hansen ML, Otis JC, Johnson JS, Cordasco FA, Craig EV, Warren RF. Biomechanics of massive rotator cuff tears: implications for treatment. *J Bone Joint Surg Am* 2008;90:316–25. <https://doi.org/10.2106/JBJS.F.00880>.
16. Henninger HB, Barg A, Anderson AE, Bachus KN, Tashjian RZ, Burks RT. Effect of deltoid tension and humeral version in reverse total shoulder arthroplasty: a biomechanical study. *J Shoulder Elbow Surg* 2012;21:483–90. <https://doi.org/10.1016/j.jse.2011.01.040>.
17. Iannotti JP, Deutsch A, Green A, Rudicel S, Christensen J, Marraffino S, et al. Time to failure after rotator cuff repair: a prospective imaging study. *J Bone Joint Surg Am* 2013;95:965–71. <https://doi.org/10.2106/JBJS.L.00708>.
18. Itoi E, Berglund LJ, Grabowski JJ, Schultz FM, Growney ES, Morrey BF, et al. Tensile properties of the supraspinatus tendon. *J Orthop Res* 1995;13:578–84.
19. Jost PW, Khair MM, Chen DX, Wright TM, Kelly AM, Rodeo SA. Suture number determines strength of rotator cuff repair. *J Bone Joint Surg Am* 2012;94:e100. <https://doi.org/10.2106/jbjs.k.00117>.
20. Kim JH, Hong IT, Ryu KJ, Bong ST, Lee YS, Kim JH. Retear rate in the late postoperative period after arthroscopic rotator cuff repair. *Am J Sports Med* 2014;42:2606–13. <https://doi.org/10.1177/0363546514547177>.
21. Kim KC, Rhee KJ, Shin HD. Arthroscopic double-pulley suture-bridge technique for rotator cuff repair. *Arch Orthop Trauma Surg* 2008;128:1335–8. <https://doi.org/10.1007/s00402-007-0527-0>.
22. Kullar RS, Reagan JM, Kolz CW, Burks RT, Henninger HB. Suture placement near the musculotendinous junction in the supraspinatus: implications for rotator cuff repair. *Am J Sports Med* 2014;43:57–62. <https://doi.org/10.1177/0363546514553091>.
23. Lee TQ. Current biomechanical concepts for rotator cuff repair. *Clin Orthop Surg* 2013;5:89–97. <https://doi.org/10.4055/cios.2013.5.2.89>.
24. Liem D, Dedy N, Hauschild G, Goshogger G, Meier S, Balke M, et al. In vivo blood flow after rotator cuff reconstruction in a sheep model: comparison of single versus double row. *Knee Surg Sports Traumatol Arthrosc* 2015;23:470–7. <https://doi.org/10.1007/s00167-013-2429-8>.
25. Matsuhashi T, Hooke AW, Zhao KD, Goto A, Sperling JW, Steinmann SP, et al. Tensile properties of a morphologically split supraspinatus tendon. *Clin Anat* 2014;27:702–6. <https://doi.org/10.1002/ca.22322>.
26. Meisel AF, Henninger HB, Barber FA, Getelman MH. Biomechanical comparison of standard and linked single-row rotator cuff repairs in a human cadaver model. *Arthroscopy* 2017;33:938–44. <https://doi.org/10.1016/j.arthro.2016.10.014>.
27. Mihata T, Gates J, McGarry MH, Lee J, Kinoshita M, Lee TQ. Effect of rotator cuff muscle imbalance on forceful internal impingement and peel-back of the superior labrum: a cadaveric study. *Am J Sports Med* 2009;37:2222–7. <https://doi.org/10.1177/0363546509337450>.
28. Miller BS, Downie BK, Kohan RB, Kijek T, Lesniak B, Jacobson JA, et al. When do rotator cuff repairs fail? Serial ultrasound examination after arthroscopic repair of large and massive rotator cuff tears. *Am J Sports Med* 2011;39:2064–70. <https://doi.org/10.1177/0363546511413372>.
29. Montanez A, Makarewich CA, Burks RT, Henninger HB. The medial stitch in transosseous-equivalent rotator cuff repair: vertical or horizontal mattress? *Am J Sports Med* 2016;44:2225–30. <https://doi.org/10.1177/0363546516648680>.
30. Park MC, Peterson A, Patton J, McGarry MH, Park CJ, Lee TQ. Biomechanical effects of a 2 suture-pass medial inter-implant mattress on transosseous-equivalent rotator cuff repair and considerations for a “technical efficiency ratio”. *J Shoulder Elbow Surg* 2014;23:361–8. <https://doi.org/10.1016/j.jse.2013.06.019>.
31. Pauly S, Fiebig D, Kieser B, Albrecht B, Schill A, Scheibel M. Biomechanical comparison of four double-row speed-bridging rotator cuff repair techniques

- with or without medial or lateral row enhancement. *Knee Surg Sports Traumatol Arthrosc* 2011;19:2090–7. <https://doi.org/10.1007/s00167-011-1517-x>.
32. Tamboli M, Mihata T, Hwang J, McGarry MH, Kang Y, Lee TQ. Biomechanical characteristics of the horizontal mattress stitch: implication for double-row and suture-bridge rotator cuff repair. *J Orthop Sci* 2014;19:235–41. <https://doi.org/10.1007/s00776-013-0504-0>.
  33. Tingart MJ, Apreleva M, Zurakowski D, Warner JJ. Pullout strength of suture anchors used in rotator cuff repair. *J Bone Joint Surg Am* 2003;85-A:2190–8.
  34. Tingart MJ, Bouxsein ML, Zurakowski D, Warner JP, Apreleva M. Three-dimensional distribution of bone density in the proximal humerus. *Calcif Tissue Int* 2003;73:531–6. <https://doi.org/10.1007/s00223-002-0013-9>.